

See discussions, stats, and author profiles for this publication at: <https://www.researchgate.net/publication/231653450>

Effects of Adhesion and Transfer Film Formation on the Tribology of Self-Mated DLC Contacts†

ARTICLE *in* THE JOURNAL OF PHYSICAL CHEMISTRY C · OCTOBER 2009

Impact Factor: 4.77 · DOI: 10.1021/jp904871t

CITATIONS

50

READS

52

3 AUTHORS, INCLUDING:



J. David Schall

Oakland University

41 PUBLICATIONS 457 CITATIONS

[SEE PROFILE](#)



Judith A. Harrison

United States Naval Academy

86 PUBLICATIONS 4,928 CITATIONS

[SEE PROFILE](#)

Effects of Adhesion and Transfer Film Formation on the Tribology of Self-Mated DLC Contacts[†]

J. David Schall, Guangtu Gao, and Judith A. Harrison*

Chemistry Department, United States Naval Academy, Annapolis, Maryland 21402

Received: May 25, 2009; Revised Manuscript Received: July 20, 2009

Diamond and diamondlike carbon (DLC) films exhibit a wide range of sometimes contradictory tribological behavior. Experimentally, isolating the influences of factors such as film structure, testing conditions, and environmental effects has proven difficult. In this work, molecular dynamics simulations were used to examine the effects of film structure, passivation, adhesion, tribochemistry, and load on the tribology of self-mated DLC contacts. Addition of hydrogen to a DLC film causes a large decrease in the unsaturated carbon bonds at the *interface* of the film when compared to both the bulk and non-hydrogenated films. These unsaturated carbon atoms serve as initiation points for the formation of covalent bonds between the counterface and the film. These adhesive interactions cause an increase in friction during sliding. The formation and breaking of covalent bonds during sliding results in the formation of a transfer film. When covalent bonds break, friction decreases and there is a concomitant increase in the local temperature emanating from the interface. These simulations reveal that reducing unsaturated atoms, both sp- and sp²-hybridized carbon, at the *sliding interface* reduces the number of adhesive interactions, alters the transfer film formed, and reduces friction. In addition, these simulations support and elucidate the passivation hypothesis for DLC friction.

Introduction

Because operating conditions such as low speeds, high loads, and extreme environments do not lend themselves to liquid lubrication of parts in moving contact, solid lubricants and surface treatments are being used in these situations.¹ Diamond-like carbon has been the subject of tremendous interest from the scientific and industrial communities due to its potential usefulness as a solid lubricant.^{2,3} Diamond-like carbon describes metastable, amorphous carbon films, with and without hydrogen, which are prepared by a variety of plasma and chemical vapor deposition techniques.^{2,3} The wide variety of ways in which DLC films can be deposited contributes to the observed large variations in film structure, mechanical properties, and tribological performance.^{3–7} DLC films exhibit a wide range of sometimes contradictory tribological behavior. For instance, friction coefficients as low as 0.003, and as high as 0.7, have been reported for various DLC films.^{8–13} Factors such as the degree of sp² and sp³ bonding, the amount of hydrogenation, and the presence of dopant atoms (e.g., Si) have a strong influence on the tribological behavior. To complicate matters even further, the overall friction can also be a function of the test conditions^{3,14} (e.g., speed, load, distance, etc.), gases present in the testing environment,^{15–21} the existence of a transfer film,^{22–24} the temperature, and the counterface material.³

Experimental evidence suggests that adhesive interactions, due to covalent bonding interactions across the sliding interface between unsaturated carbon atoms, are one of the major sources of friction in DLC.^{3,25,26} For example, ultrahigh vacuum (UHV) tribometer experiments of sliding bearing steel pins against hydrogenated amorphous carbon (a-C:H) coated silicon wafers have measured very low friction coefficients in the range 0.01–0.001 after a short run-in period.^{27,28} After a brief period of low friction, in as few as 1–15 cycles, a dramatic increase

in friction coefficient to the 0.1 range occurred.²⁶ In films with higher hydrogen content, the increase in friction was delayed. When hydrogen was added as a background gas in the UHV tribometer, superlow friction was restored after transient high friction events.²⁶ It was shown that a minimum hydrogen pressure of 100 Pa was required to restore superlow friction and that increased hydrogen pressure delayed the onset of, and lowered, the friction maximum. From these experimental observations, it was inferred that hydrogen passivated the unsaturated carbon atoms at the film surface. It was also hypothesized that when films have high hydrogen content, free hydrogen within the film migrates to the sliding interface, prolonging the initial low-friction regime by providing additional passivation. As wear removes hydrogen from the surface, the hydrogen reservoir within the film is thought to be depleted, and friction increased. By providing hydrogen as a background gas, it is assumed that the surface passivation was continually replenished. The concept of adhesion and surface passivation by hydrogen is neither new nor unique to DLC. Similar hypotheses have been made for self-mated diamond contacts²⁹ and ultrananocrystalline (UNCD) diamond.^{30,31}

The hypothesis that passivation of diamond and DLC surfaces with hydrogen reduces friction is supported by several recent experiments,^{30–34} by MD simulations,^{35–38} and more recently by density functional theory.³⁹ For example, the macroscopic friction coefficient of hydrogenated DLC was recently investigated in UHV under partial pressures of water vapor, oxygen, nitrogen, and hydrogen. After run-in, the friction decreased and increased again during longer duration tests. The increase in friction was accompanied by hydrogen desorption as measured by mass spectrometry.³² Nanoscale measurements have shown that the adhesion and friction of UNCD are both reduced after hydrogen termination.^{30,31} MD simulations have shown that the removal of hydrogen atoms from diamond surfaces in normal contact leads to increased chemical bond formation, or adhesion. In that case, covalent bonds were formed across the interface

[†] Part of the “Barbara J. Garrison Festschrift”.

* Corresponding author. E-mail: jah@usna.edu.

and separation of the surfaces led to fracture. Similarly, removing the hydrogen termination from a diamond counterface increases friction when it is in sliding contact with DLC by increasing the formation of chemical bonds between the counterface and the DLC.³⁶

Hydrogenated amorphous carbon (a-C:H) has shown particular promise as a solid lubricant.^{3,27,28,40} These films contain approximately 20–60 atomic percent hydrogen and have a range of sp³-to-sp² ratios between 1:3 to 9:1. Hydrogenated amorphous carbon films have unique properties, which make them ideal solid lubricants. For instance, they are strain tolerant, are compressible, and have some self-healing ability, all of which improve wear resistance. Films of a-C:H also have a tendency to react with the counterface material forming a transfer layer, a new material formed due to tribochemistry. It has also been speculated that the low friction after run-in of diamond and polycrystalline diamond films is due to the formation of a transfer layer, possibly graphitic in nature.⁴¹ In contrast, recent examination of UNCD wear tracks with NEXAFS and X-PEEM have concluded that the lubrication mechanism of UNCD does not involve the formation of graphite or amorphous carbon under a broad range of conditions.⁴²

Transfer films are known to play an important role in the friction of dry sliding contacts.^{22,43,44} Particles that are detached from the surfaces in sliding contact can act as a physical barrier, separating the surfaces, or can undergo sliding induced chemical reactions to a material that is chemically distinct from the siding surfaces. Recently, several experimental methods have been developed to observe interfacial sliding in solid–solid contacts.^{45–48} For example, the formation and thickness of carbon transfer films when a sapphire hemisphere was in contact with a diamondlike carbon coating has been observed with video microscopy while the composition of the films has been quantified with Raman spectroscopy.^{22,43,44}

Experimental elucidation of the role of hydrogen in surface passivation and the influence of transfer film formation on the friction of DLC is complicated by the fact that it can be difficult to isolate the influence of these factors on adhesion and friction. For instance, the prevalence of unsaturated carbon sites at the sliding interface of a DLC film is a function of the structure of the bulk DLC and the deposition conditions. Once the film is made, and during testing, exposure to environmental gases can have an influence on availability of unsaturated surface sites. Finally, testing conditions, such as sliding speed, load, environmental gases and counterface identity, can result in the passivation of unsaturated sites, the creation of new sites, and the formation of transfer films. The complicated interplay between the factors that influence DLC friction underscores the need to understand the fundamental atomic-scale processes that govern this interplay.

Molecular dynamics (MD) simulations are uniquely suited to elucidate the influence of all the factors that affect DLC friction because the positions and velocities of all atoms are known as a function of time. Previous MD simulations have examined the friction between diamond (111)(1×1)-H surfaces in sliding contact with two separate hydrogen-free a-C films with different thicknesses.³⁶ Because the films had similar interfacial structures, they exhibited similar tribological behavior. Above a critical load, a series of tribochemical reactions occurred in the films. These reactions caused significant restructuring and a lowering of friction, which was consistent with run-in behavior observed in DLC friction experiments. MD simulations have also shown that the three-dimensional structure, not just the sp³-to-sp² carbon ratio, is critical in determining

the mechanical properties of the amorphous carbon films. Orientations of sp²-ringlike structures perpendicular to the film surface resulted in films with both high sp² content and large elastic constants, whereas films with sp²-ringlike structures parallel to the film surface had small elastic constants.

An understanding of the atomic-scale friction of self-mated DLC systems is particularly important for the use of DLC as a solid lubricant in MEMS devices. To that end, MD simulations were used to examine the friction as a function of load between a hydrogen-terminated amorphous carbon surface and amorphous carbon surfaces with and without hydrogen incorporation. Preliminary results showed that hydrogen incorporation into the amorphous carbon films can reduce friction.^{49,50} In this work, we revisit the friction between self-mated, amorphous carbon systems by conducting simulations aimed at elucidating the role hydrogen incorporation within the film plays in changing the *interfacial* film structure, the role it plays determining the nature of tribochemical reactions between film and counterface, the mechanism of transfer layer formation, changes in film structure *during sliding*, and temperature changes that occur during sliding.

Method

The simulation systems consist of a hydrogen-terminated amorphous carbon counterface brought into sliding contact with samples of amorphous carbon films attached to diamond (111) substrates. The substrates contain seven layers of carbon atoms with 144 atoms per layer. Periodic boundary conditions are applied in the plane parallel to the sliding interface. The dimensions of the computational cell in the sliding plane are 30.2 by 26.1 Å, which corresponds to twelve diamond unit cells repeated along the [110] lattice direction and six unit cells repeated along the [112] lattice direction, respectively. The sliding direction is the [110] direction of the underlying diamond substrate. The top two layers of the counterface and bottom two layers of the film are held rigid. Loading of the counterface onto the film is accomplished via a constant-load algorithm,⁵¹ which mimics a real constant load experiment. A constant normal force is applied on the tip. Governed by Newton's laws, the tip oscillates slightly around an equilibrium separation above the film producing an average load on the film equal to the constant normal force on the tip. This algorithm reproduces the experimental equivalent of a constant-load. To model sliding, a constant velocity of 0.902 Å/ps (90.2 m/s) is applied to the rigid layers of the counterface in the sliding direction. The sliding velocity is chosen so that the counterface makes exactly six complete passes over the film in 200 ps of simulation time. A number of research groups have investigated friction as a function of sliding speed for various simulation systems and have found the results to be largely invariant over the range of computationally accessible sliding speeds.^{52,53} Moving inward toward the interface, the next two layers of the film and counterface are maintained at a constant temperature of 300 K via a generalized Langevin thermostat.^{54,55} All the remaining atoms are free to move according to classical dynamics. The equations of motion for all nonrigid atoms are integrated using the velocity–Verlet algorithm⁵⁶ with a constant time step of 0.25 fs.

Interatomic forces are modeled by Brenner's second-generation reactive empirical bond-order potential (REBO).⁵⁷ The parameters and the functional form of this updated REBO were altered so that the potential more accurately reproduces the elastic constants of diamond and graphite, while not disrupting the properties that were fit in the earlier version of the

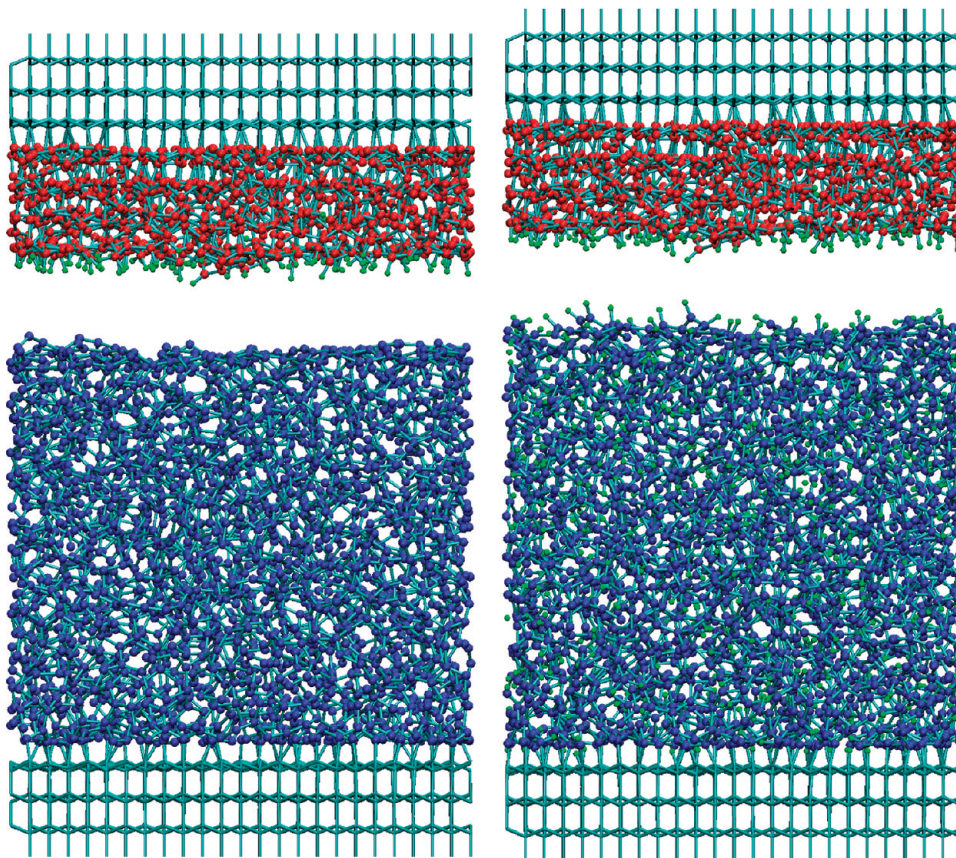


Figure 1. Initial configurations of the (a) non-hydrogenated and (b) hydrogenated amorphous carbon films and counterface (shown above the film in each figure). Film carbon and counterface carbon atoms are blue and red, respectively. Hydrogens are green. The diamond substrate is also shown. In the reference frame of the simulation, x , y , and z are along the $[\bar{1}10]$, $[\bar{1}\bar{1}2]$, and $[111]$ directions of the underlying diamond support structure. The counterface moves from left to right along the $[\bar{1}10]$ direction during sliding.

potential.^{58,59} This potential energy function, and its predecessor, have been used to model mechanical properties in filled⁶⁰ and unfilled⁶¹ nanotubes, properties of clusters,⁶² the tribology of diamond^{63–69} and DLC,^{35,36,50} and stress at grain boundaries.^{70,71} The REBO analytically describes energies and forces of various solid structures of carbon as well as hydrocarbon molecules as a function of local coordination, types of neighboring atoms, and the degree of conjugation. The many-body nature of the REBO potential allows the bond energy of each atom to depend on its local environment. Therefore, REBO is one of a few empirical potentials that allows for chemical reactions and the accompanying changes in bond-hybridization. In the context of tribology, reactivity means that wear events can be simulated. Zhang et al.³⁴ recently reported results of molecular dynamics simulations of the tribology of hydrogenated amorphous carbon. In their study, forces within the film and counterface were modeled using Brenner's first generation REBO potential.^{58,59} Interfilm forces, i.e., forces between the film and counterface, were modeled using a long-range, Lennard-Jones (LJ) potential. The LJ potential does not allow for chemical reactions to occur between the film and counterface. Therefore, one of the factors affecting friction in amorphous carbon, namely the formation of adhesive bonds between film and counterface, was not incorporated into their study. Long-range intermolecular forces were added to the second-generation REBO potential by using a novel adaptive algorithm to maintain the reactive nature of the potential energy function.⁷² Results of friction simulations for a number of different tribosystems demonstrated that the same qualitative trends are produced in the data when the REBO and AIREBO potentials are used.³⁶ There are two differences

that should be noted, however. Higher normal forces are required to produce the same friction force with AIREBO³⁶ and the error bars associated with average friction forces obtained using AIREBO are noticeably smaller. The magnitude of the fluctuations in the LJ forces at the interface is smaller than fluctuations in covalent forces.⁵⁰ The qualitative trends are the same with both potentials and the computational time required for simulations with REBO is significantly less. With these things in mind, the REBO potential is used here.

It is straightforward to develop a data set that facilitates analyses for model nonwear counterface–film systems.⁵⁰ In these systems, each atom is a member of either the set of counterface atoms or the film atoms with its membership being maintained throughout the course of the simulation. In contrast, when reactions take place between the film and counterface, the membership of a given atom changes during the course of the simulation. In light of this, the normal and friction forces reported here are determined by summing the appropriate components of the forces on atoms in the rigid counterface atoms not by examining contact forces on interfacial atoms.

To study the influence of hydrogen content on adhesion, transfer film formation, and friction in amorphous carbon films, a non-hydrogenated and a hydrogenated film were created (Figure 1). The non-hydrogenated and hydrogenated films contain 0 and 20 at. % hydrogen, respectively. Experimentally, amorphous carbon films are made by vapor deposition techniques, where the technique and deposition process control the structure of the film. Films can be generated by reproducing the entire deposition process via molecular dynamics simulation; however, this is not a computationally efficient way to produce

TABLE 1: Film Composition and Properties

film identity	total C	total H	sp (%)	sp ² (%)	sp ³ (%)	thickness (Å)	C _{zz} (GPa)	surface roughness, rms (Å)	density (g/cm ³)
0 at. % H	3000	0	2.2	85.3	12.5	29.7	358.7	0.57	2.75
20 at. % H	3000	750	2.1	83.4	14.5	27.6	295.4	0.71	2.40
top 2 Å of 0% H film (interface)			18	76	6				
top 2 Å of 20% H film (interface)			5	87	8				
counterface	1115	120	0	5.6	94.4	10.1	462	0.48	2.86

films with differing properties.^{34,73–75} Two other widely used simulation methods for creating amorphous carbon films are homogeneous condensation of a vapor and ultrafast quenching of liquid carbon.^{76–81} The amorphous carbon films examined here are generated by randomly placing carbon C (and H) between a hydrogen-terminated and an unterminated diamond (111) surface and heating to 8000 K. After the melt is equilibrated, the systems are rapidly quenched to 800 K using an exponential quench rate of the form $T = 8000 \exp(-c dt)$. The constant c was chosen such that cooling takes approximately 2 ps. The system was then brought to its minimum energy configuration via a steepest descent algorithm and equilibrated at 300 K. The resulting structures exhibit multiple bonds between the film and unterminated diamond interface, which is now the substrate, and a relatively smooth surface at the hydrogen-terminated diamond interface. Rapid quenching ensures that the bulk of the hydrogen does not migrate to the interface between the amorphous carbon and hydrogen-terminated diamond surface. This method leads to nonlayered films with high sp²-hybridized carbon content and low densities. Slower quenching results in layered films.³⁵ After quenching and equilibration, the hydrogen-terminated diamond surface above the DLC film is removed and replaced with the counterface (Figure 1). The bulk properties of the films are summarized in Table 1. The structure and composition of the non-hydrogenated and hydrogenated films closely resemble that of a-C and a-C:H, respectively.⁸² The nature of the interface has a significant influence on the observed friction. With that in mind, the top 2.0 Å of both the hydrogenated and non-hydrogenated films were characterized (Table 1). Examination of these data reveals that the interface has a larger fraction of unsaturated sp-hybridized carbon atoms than the bulk film. In addition, the non-hydrogenated film has a much larger fraction of sp-hybridized carbon in the interfacial region than the hydrogenated film.

To facilitate analysis and ease comparison, each sliding simulation is conducted using the same counterface. The counterface used here was generated previously (referred to therein as film IV) and has been well characterized.³⁵ This film was generated in a way similar to that of the two films described above with two notable exceptions. The quenching rate was on the order of 100 ps and the first-generation REBO potential was used. Because the quench rate was relatively slow, the majority of the hydrogen migrated to the surface of the film, effectively passivating it. The properties of the counterface are also summarized in Table 1. The structure and composition of the counterface resembles that of t-aC.⁸² The choice of this particular film as the counterface was made because it exhibits high compressive modulus and high sp³-carbon content and has a relatively smooth interfacial surface with a high degree of hydrogen termination.

Results

Friction. The counterface slides over the film six times for a total sliding distance of 180.4 Å in all the simulations. Each

pass takes approximately 33 ps of simulation time. Instantaneous forces on the rigid-layer atoms were saved every 0.1 ps. The smoothed,⁸³ instantaneous friction force as a function of sliding distance has been plotted in Figure 2a for the non-hydrogenated and hydrogenated films under a normal load of 90 nN. At this load, the hydrogenated film shows lower friction force at all times during the simulation. This is typical behavior and is generally observed at all loads. The average friction force versus average normal force for each sliding simulation is shown in Figure 2b. The average friction and normal forces are obtained by averaging over the final pass of the counterface over the film where it appears that the friction force oscillates around a steady-state value. Error bars represent the standard deviation of the friction and normal force during the final pass of the counterface over the film. The hydrogenated system shows lower friction force at each load, with the greatest reduction in friction being at low to moderate loads (<60 nN). At the highest loads investigated (>90 nN), the friction force of the hydrogenated system approaches that of the non-hydrogenated system. These results are consistent with our previous results for hydrogen-terminated and partially hydrogen-terminated diamond (111) in sliding contact with DLC, which indicated that friction is largely dependent on the degree of hydrogen termination present.³⁶ In light of that, friction was expected to be significant in the case of the non-hydrogenated film due to the unsaturated carbon atoms at the interface. In fact, the threshold load for tribocochical reactions between non-hydrogenated film and counterface is below 10 nN, the lowest load examined. The hydrogenated film contains a small amount of trapped H₂. However, during the time scale of the simulation it does not diffuse to the sliding interface and has no effect on the friction.

The usefulness of MD simulations lies in the wealth of atomic-scale information they provide, information that is unavailable from experiment. Quantities that remain difficult to measure experimentally include the number and type of chemical reactions that occur during sliding and the local temperature at all points in the system during sliding. Creative exploration of these and other quantities can provide a unique window into understanding properties that are measured experimentally.

Structure. Visual inspection of the equilibrated simulation systems in Figure 1 reveals the inclusion of hydrogen into the amorphous carbon film appears to roughen the surface of the film. To quantify this roughness, constant potential energy topographic plots of the films and the counterface were created (Figure 3). These plots are created by orienting a hydrogen molecule perpendicular to the film surface. The distance of the molecule from the surface of the film is adjusted until the potential energy of the system reaches a predetermined, fixed value. The molecule is rastered over the film to calculate the constant potential-energy distance at all points. While all the films have high and low points, the hydrogenated film is characterized by an abundance of deep holes and areas with high atoms. The distance data as a function of surface position can also be used to calculate an rms roughness (Table 1). The

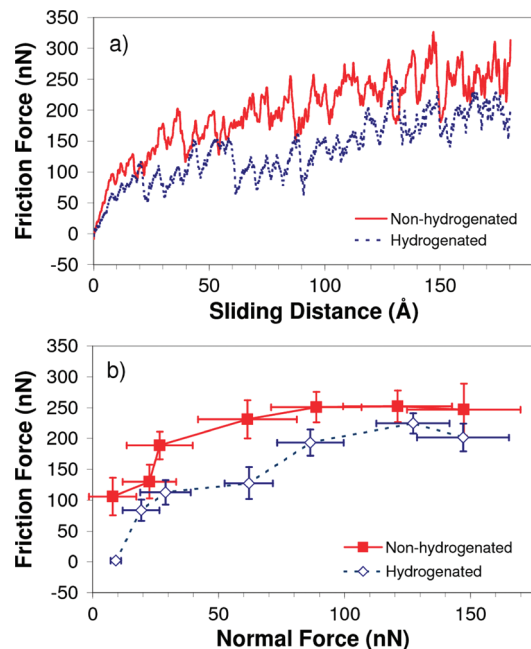


Figure 2. (a) Friction force as a function of sliding distance for each system with an average normal force of 90 nN. The data have been smoothed using a standard smoothing function. (b) Average friction force as a function of average normal force.

rms roughnesses reveals that the counterface is the smoothest, while the hydrogenated film is the roughest.

To determine the degree of saturation and to track tribocatalytic reactions, the coordination number for each carbon atom in the system was calculated using the following equation

$$C_i = \sum_{j \neq i} f_{ij}^c \quad (1)$$

where f_{ij}^c is the cutoff function from the interatomic potential between atom i and all other atoms j . The cutoff function is a continuous piecewise function of radial distance from atom i , which varies smoothly between one, for atoms within the interaction range of the potential, and zero, for atoms outside the range of interaction. The form and parameters for the cutoff function used in this analysis are the same as the interatomic potential,⁵⁷ which is capable of tracking partial neighbors and transition states. A coordination number of 4 indicates that carbon is fully saturated (sp^3 -hybridized), while a number less than 4 indicates unsaturation. Before sliding, the average coordination number of the carbon atoms in the 2.0 Å of the non-hydrogenated and hydrogenated films closest to the interface is 2.88 and 3.03, respectively. For comparison, the average coordination number in the first 2.0 Å of the hydrogen-terminated counterface is 3.50.

The number of film–counterface carbon–carbon (C–C) bonds formed in 1 ps intervals throughout the simulation for the non-hydrogenated system and the hydrogenated system at normal forces of 10, 60, and 150 nN are shown in Figure 4a,b, respectively. It is clear from analysis of Figures 4 and 2 that the number of cohesive bonds between the film and counterface directly impacts to the average friction force. The number of interfilm bonds increases with increasing normal force while presence of hydrogen in the film reduces the number of interfilm bonds. The number of interfilm bonds between the non-hydrogenated film and counterface is approximately equal for

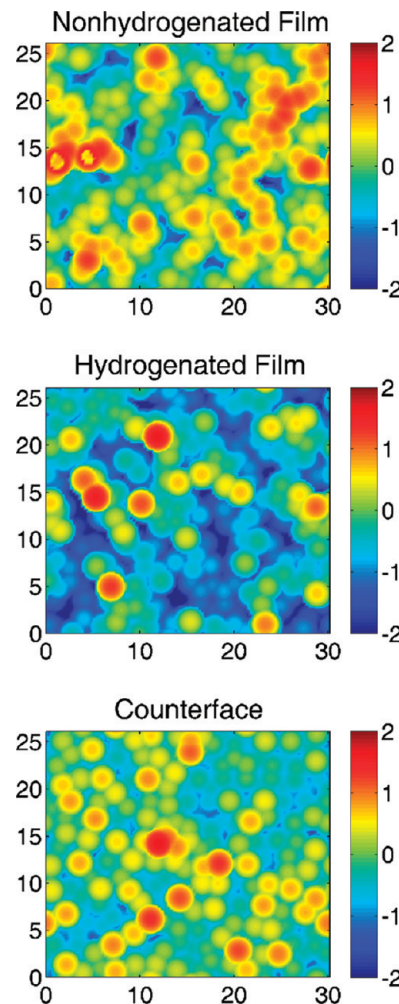


Figure 3. Constant potential energy, topographic maps of the two films and counterface used here. The scale (color bar) represents the distance in Å above the surface of a hydrogen molecule. The distance of the molecule is adjusted until the desired potential energy is achieved.

all loads above 60 nN. As a result, the average friction force shows a plateau-like behavior above 60 nN, as shown in Figure 2b. At any given load, the hydrogenated system has significantly fewer interfilm C–C bonds compared to the non-hydrogenated system. To illustrate this point, the number of C–C bonds between atoms initially identified as belonging to the film and those initially identified as belonging to the counterface was tallied. An exact number of bonds across the interface between the film and counterface is difficult to determine because of mixing and shear of film and counterface atoms at the interface. At a load of 60 nN, a total of 3675 C–C bonds are formed between the carbon atoms in the non-hydrogenated film and the counterface by the end of the simulation. In contrast, only 1130 C–C bonds form between the carbon atoms in the hydrogenated film and counterface during the course of sliding.

Significant rearrangements of the carbon atoms in the region of the interface occur, particularly at high loads, or when the hydrogen content is low. Because the counterface has a large fraction of sp^3 -hybridized carbon atoms, these rearrangements tend to increase the number of unsaturated carbon atoms. When a large number of interfilm bonds form, significant mixing of the film and counterface atoms occurs (Figure 5). The left-hand side of Figure 5 contains snapshots of the system configuration of the non-hydrogenated system under a normal force 60 nN before and after sliding. Atoms are colored according to their

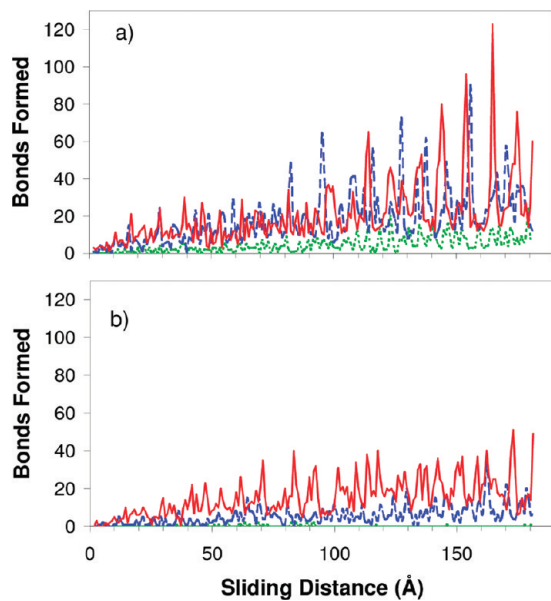


Figure 4. Number of new C–C bonds between the film and counterface formed during 1 ps intervals over the course of the simulation for (a) the non-hydrogenated film and b) the hydrogenated film. Normal forces are 10 nN (green short-dashed line), 60 nN (blue long-dashed line), and 150 nN (red solid line).

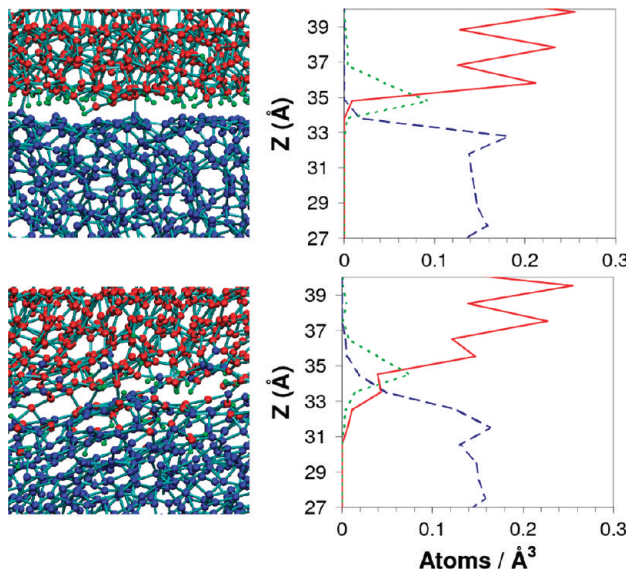


Figure 5. Atomistic snapshots (left) of the non-hydrogenated film and corresponding atomic density plots (right) shown before (top) and after 200 ps of sliding (bottom). Film carbon atoms are blue, counterface carbon atoms in red, and counterface hydrogen atoms in green. The atomic density of film carbons, counterface carbons, and counterface hydrogens are indicated by blue long dashed lines, red solid lines, and green short dashed lines, respectively. The applied load is 10 nN.

initial attachment point. Carbon atoms that belong to the film and those that belong to the counterface are blue and red, respectively. The hydrogen atoms originally attached to the counterface are green. The right-hand side of Figure 5 shows the density of atoms according to their position along the z -axis of the simulation (the vertical direction as shown in Figure 1) before and after sliding. The same color coding is used in these plots to indicate film carbon, counterface carbon, and counterface hydrogen. Before sliding, there is little overlap of the colored lines in Figure 5. Thus, there is little mixing of the film and counterface atoms, although several C–C bonds are apparent between the film and counterface. As sliding progresses,

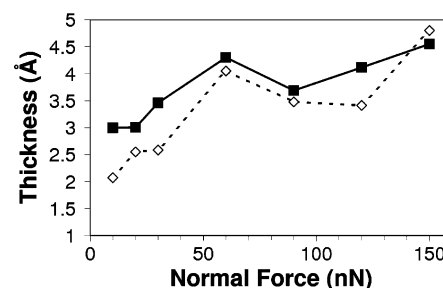


Figure 6. Transfer layer thickness as a function of load for the non-hydrogenated (solid squares) and hydrogenated (open diamonds) films.

mixing of the film and counterface atoms is visible in the atomistic snapshot and there is a significant overlap of the lines of the atomic density plots in the interface region (initially located at ~ 34 Å).

When tribochemical reactions occur during sliding, a transfer film can be formed.¹ Recent experiments have demonstrated that it is possible to measure the thickness of these films.^{22,44,84} To estimate the transfer layer thickness formed during sliding, the maximum extent of atom transfer, as indicated by the measure of overlap of the atomic densities of the film and counterface carbon atoms, is divided by 2. The underlying assumption is that if the film and counterface were separated, half the transfer layer would adhere to the film and half would adhere to the counterface. The transfer layer thickness for the hydrogenated (open diamonds) and non-hydrogenated (closed squares) systems is shown in Figure 6. In both systems, the transfer layer thickness increases with increasing load. In general, the hydrogenated system has a thinner transfer layer than the non-hydrogenated system, particularly at low loads.

To determine the structure of the interface and how it evolves during sliding, the coordination number for each carbon atom in the system was calculated. The system was divided along the z -direction into 200 equally spaced bins, approximately 0.25 Å thick, and then the average coordination number for all carbon atoms contained in each bin was determined at 1 ps intervals during the simulation. The average coordination number can then be displayed as a function of z -coordinate and simulation time for any given sliding simulation (Figure 7). The average coordination number for bins in the diamond substrates is not shown. At the beginning of each simulation, a clear boundary between the film and counterface atoms is apparent at approximately 34 Å in both the non-hydrogenated and hydrogenated systems. The film contains mostly 3-fold coordinated (sp^2 -hybridized) carbon atoms, while the counterface contains mostly 4-fold coordinated (sp^3 -hybridized) carbon. As the counterface slides over the non-hydrogenated film, the average coordination number of the counterface is reduced to 3, with a significant drop around 105 ps of simulation time. By the end of sliding, the majority of the carbon atoms in the counterface convert from 4-fold to 3-fold coordination. In contrast, the boundary between the hydrogenated film and the counterface remains fairly distinct and the counterface carbon atoms remain mostly sp^3 -hybridized, except for a thin layer near the interface, which appears to be rich in sp^2 -hybridized carbon.

To further quantify the structure, the relative bond angle distribution was calculated every 0.2 ps during the simulation. An initial bond angle distribution was calculated from the system configuration prior to sliding and subtracted from subsequent distributions determined while sliding so that changes in bond angles could be determined. The resulting change in bond angle

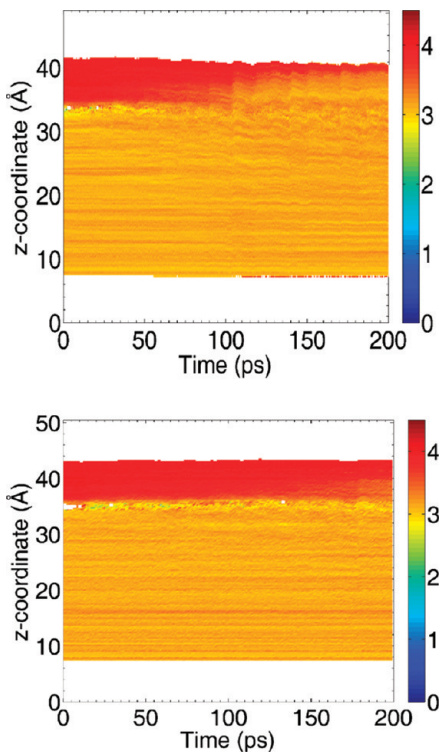


Figure 7. Coordination number for carbon atoms as a function of position normal to the loading axis (y -axis) and time (x -axis) for the non-hydrogenated (top panel) and hydrogenated films (bottom panel). The normal load is 60 nN. The coordination number is indicated by the color bar.

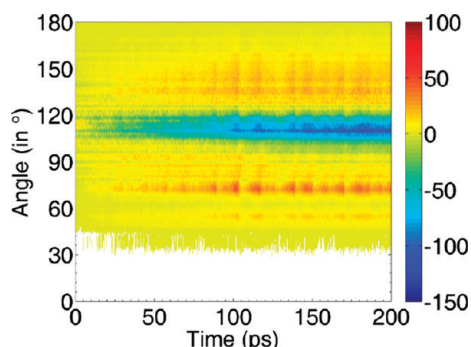


Figure 8. Change in bond angle distribution as a function of simulation time for the non-hydrogenated film when the load is 60 nN. The change in the number of bonds with a given bond angle is indicated by color scale at the right of each figure.

distribution is shown for the non-hydrogenated film in Figure 8. There is a notable depletion of bond angles in the range around 109.5° (i.e., the appearance of the blue region), which is consistent with the depletion of sp^3 -hybridized carbon atoms in the counterpart. A depletion also occurs in the hydrogenated film; however, the magnitude of the depletion is greatly reduced. There appears to be a fairly periodic buildup of the number of bonds with angles below 75° and above 130° followed by a rapid decrease, indicated by the red and yellow striping (Figure 8). A visual inspection of atomistic snapshots indicates the formation of three-membered rings, as illustrated in Figure 9, which form at 89.6, 97, and 97.6 ps. They break almost simultaneously between 102.6 and 102.8 ps. The temperature profile of the non-hydrogenated system as a function of sliding time at a load of 60 nN is shown in Figure 10. For reference, the friction force data for the non-hydrogenated system has been replotted as a function of simulation time. The structure of the

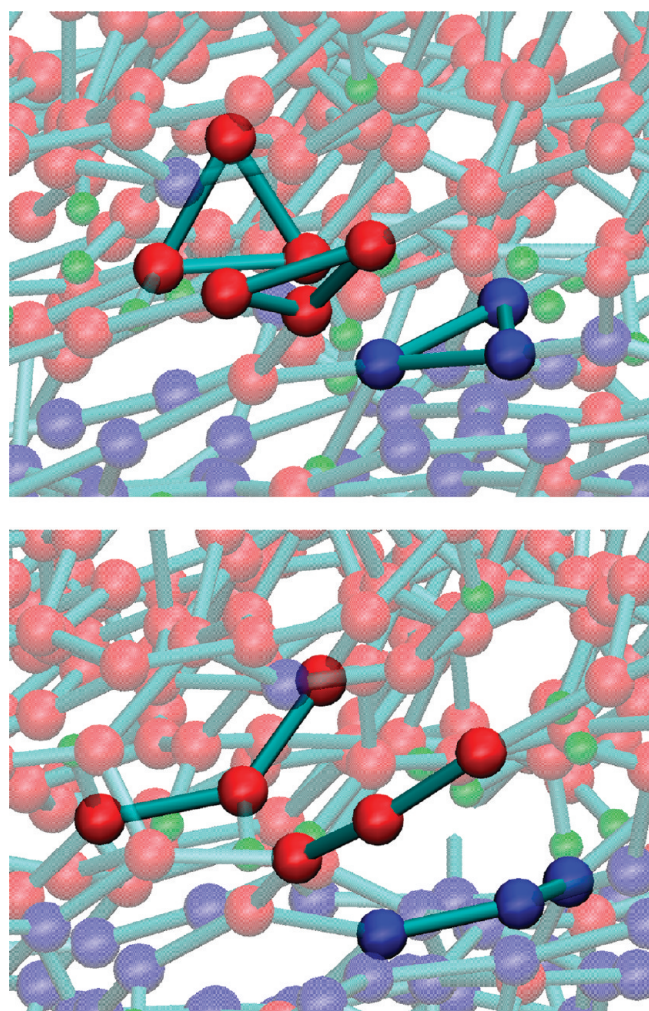


Figure 9. Atomistic snapshots of the non-hydrogenated film at the sliding time of 102 ps (upper panel) and 103 ps (lower panel) when the load is 60 nN. The highlighted rings were formed at 89.6, 97, and 97.6 ps. The bonds break almost simultaneously between 102.6 and 102.8 ps. Film and counterpart atoms are colored by the same convention used in Figure 1.

transfer film, or the interfacial region, is continually changing during sliding. The spikes in temperature correspond to the breakdown of structures such as the three-membered rings pictured in Figure 10. Each temperature spike also corresponds to a drop in the friction force, which indicates that the scission of covalent bonds. The associated vibrational excitation this causes contributes to the increase in temperature. The non-hydrogenated system experiences much higher interface temperatures than the hydrogenated system. At 60 nN normal force, in a 2.5 Å thick section containing interface between the film and counterpart, the average interface temperatures are 826 ± 287 and 582 ± 146 K, for the non-hydrogenated and hydrogenated systems, respectively. The second generation REBO potential is known to overpredict the heat of formation for tricyclic compounds.⁵⁷ For example, ab initio calculations predict the heat of formation of cyclopropene to be 68.3 kcal/mol, whereas, REBO predicts a value of 98.71 kcal/mol. For the decomposition reaction of cyclopropene to methylacetylene, a reaction somewhat analogous to that illustrated in Figure 9, ab initio calculations predict the release of 22.5 kcal/mol of energy, whereas REBO predicts 47.24 kcal/mol will be released. While this energy difference is likely to affect the magnitude of the temperatures observed, the relative trends in temperature dif-

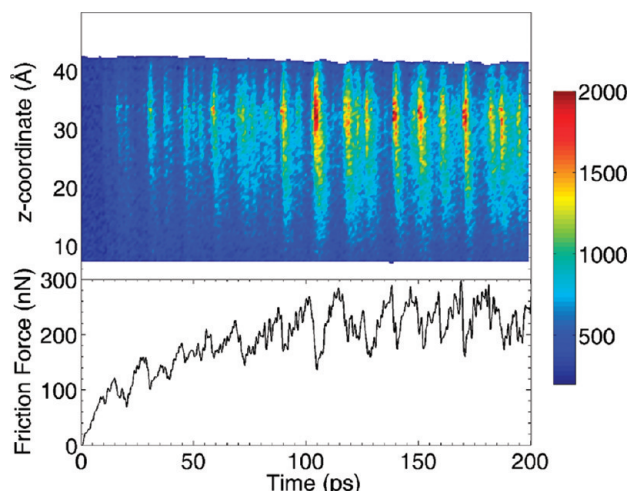


Figure 10. Temperature profile along the loading axis as a function of time for the non-hydrogenated film when the load is 60 nN. The system was divided into 200 bins approximately 0.25 \AA thick, and the average temperature of the atoms contained in each bin was determined every 0.2 ps. For ease of comparison, the friction force for the non-hydrogenated film from Figure 2 has been replotted.

ferences between the hydrogenated and nonhydrogenated films should not be affected.

Discussion

Diamondlike carbon has long been known to exhibit a wide range of tribological properties. In a recent review,³ the major causes of friction in DLC were categorized into five areas: (1) physical and mechanical interactions, (2) adhesive interactions, (3) tribochemical interactions, (4) thermal interactions, and (5) third-body interactions. The large number of factors affecting DLC friction, coupled with the fact that a complex interplay exists among these factors, makes the elucidation of the underlying mechanisms governing DLC friction difficult. In this work, MD simulations were used to examine the complex interplay between hydrogen content, passivation, adhesion, transfer film formation, temperature, and friction at the atomic scale.

Previous MD simulations that examined two hydrogen-free films with different thicknesses, but similar interfacial structures, showed that the structure of the film near the interface played a crucial role in determining the tribological response of those films.³⁶ In this work, both the bulk and interfacial structure of each film was examined. In the bulk, the hydrogenated and non-hydrogenated films have approximately the same percentages of sp-, sp²-, and sp³-hybridized carbon atoms. In contrast, the composition of the interfacial region of both films confirms that there are significantly more unsaturated carbon atoms at the interface than in the bulk. In addition, the incorporation of hydrogen dramatically reduces the number of unsaturated sp-hybridized carbon atoms at the interface. These structural differences underscore the need to characterize the interfacial structure of DLC for use in tribological applications in addition to the bulk composition.

Careful analysis of the bonds formed and broken at the interface during sliding revealed that the unsaturated carbon atoms, both sp-hybridized and sp²-hybridized, near the interface serve as initiation points for the formation of carbon–carbon bonds between the counterface and the film (interfilm bonds). This increase in interfilm bonds increases the adhesive interactions between the film and the counterface. As a result, the

friction increases. These findings are consistent with the passivation hypothesis put forth to explain the low friction of diamond^{85–88} and DLC^{2,3,15,25–27,29,89} in air, compared to vacuum, and in the presence of hydrogen or water. These conclusions are also consistent with early MD simulations that showed the adhesion, or the formation of covalent bonds, between two diamond (111) (1×1)-H surfaces and a diamond tip and a diamond (111)(1×1)-H surface, increases if hydrogen is removed from the surfaces.^{38,90} Subsequent DFT simulations of diamond adhesion yielded similar findings.³⁹ The formation of covalent bonds between a diamond(111)(1×1)-H counterface and a hydrogen-free DLC during sliding also increases when hydrogen is systematically removed from the counterface.³⁶ Recently, spectroscopic evidence for the passivation hypothesis was obtained by using NEXAFS to examine the wear tracks in UNCD in the presence of water vapor.⁴² In addition, amorphous sp²-hybridized carbon was also formed in the UNCD wear track. In the simulations presented here, while sp²-hybridized carbon was formed, no evidence of graphite-like rings was observed.

Macroscopic experiments have recently shown that when a sapphire ball is in sliding contact with a DLN film (diamondlike nanocomposite) carbon-containing transfer films tens to hundreds of nanometers thick can be formed.^{22,44} These experiments are unique because the thickness of the transfer film was monitored during sliding. This allowed for correlations between thinning of the transfer film and concurrent friction spikes to be made. While this experiment provided important information regarding the thickness of the transfer film during sliding, it provided no information related to the atomic-scale mechanism of transfer film formation. Indeed, while some progress has been made observing atomic-scale events at buried interfaces,^{47,48} this remains one of the foremost challenges for tribologists.⁴⁵ Because it is possible to track the positions of all atoms during sliding in MD simulations, atomic-scale changes that occur at the sliding interface can be elucidated. The simulations discussed herein reveal that the formation of carbon–carbon bonds, initiated by the presence of unsaturated interfacial carbon atoms, between the counterface and the film lead to significant changes at the interface. By tracking the origination point of the carbon atoms, we developed a method to estimate the thickness of transfer films formed in the simulation. The thickness of the transfer films increased with increasing load for both hydrogenated and non-hydrogenated films. Decreasing the number of unsaturated carbon bonds at the interface, by adding hydrogen, decreased the thickness of the films compared to the hydrogenated films at all but the highest load examined.

Friction is the dissipation of energy. In diamond and DLC where electronic friction is likely to be negligible, the major mechanisms of energy dissipation are wear and the dissipation of heat via phonons. Atomic-scale “stick–slip” has been measured with the atomic force microscope on diamond surfaces. The slip has been termed “plucking”, which leads to vibrational excitation of the solid. This energy is then dissipated via phonons. Previous MD simulations examined the wearless friction between two diamond (111)(1×1)-H surfaces⁶⁹ and two diamond (001)(2×1)-H surfaces⁹¹ in sliding contact. In both cases, maxima in the friction force corresponded to points of strong interaction between opposing hydrogen atoms. When the surfaces slipped past one another, the friction decreased and the surface carbon–hydrogen bonds were vibrationally excited. The simulations presented herein are not in the wearless friction regime. Despite this, insight into energy dissipation was gained. When interfilm reactions occur, the friction force increases during sliding due to the formation of covalent bonds. Continued

sliding increases the stress on the covalent bonds in the interfacial region until these bonds break. When the bonds break, the friction force decreases suddenly. Thus, the friction force as a function of sliding distance is periodic in the majority of these simulations, but the periodicity does not arise from the structure of the underlying substrate, rather it coincides with the buildup and breaking of covalent bonds. The severing of the chemical bonds also contributes to the vibrational excitation of the counterface and film atoms, which is manifest as temperature spikes that emanate from the interface and extend into the counterface and the film.

Acknowledgment. J.D.S. and G.A.O. acknowledge support from AFOSR under contract F1ATA09086G002 and as part of the Extreme Friction MURI, respectively. J.A.H. also acknowledges support from the ONR (N0001409WR20155) and AFOSR.

References and Notes

- (1) Singer, I. L. Mechanics and chemistry of solids in sliding contact. *Langmuir* **1996**, *12*, 4486–4491.
- (2) Erdemir, A.; Donnet, C. Tribology of Diamond, Diamond-Like Carbon, and Related Films. In *Modern Tribology Handbook*; Bhushan, B., Ed.; CRC Press LLC: Boca Raton, FL, 2001; Vol. 2, pp 871–908.
- (3) Erdemir, A.; Donnet, C. Tribology of diamond-like carbon films: recent progress and future prospects. *J. Phys. D-Appl. Phys.* **2006**, *39* (18), R311–R327.
- (4) Robertson, J. Diamond-like amorphous carbon. *Mater. Sci. Eng., R* **2002**, *37*, 129–281.
- (5) Robertson, J. Electronic and atomic structure of diamond-like carbon. *Semicond. Sci. Technol.* **2003**, *18*, S12–S19.
- (6) Hainsworth, S. V.; Uhure, N. J. Diamond like carbon coatings for tribology: production techniques, characterisation methods and applications. *Int. Mater. Rev.* **2007**, *52* (3), 153–174.
- (7) Robertson, J. Amorphous-Carbon. *Adv. Phys.* **1986**, *35* (4), 317–374.
- (8) Erdemir, A.; Fenske, G. R. Tribological Performance of Diamond and Diamond-Like Carbon Films at Elevated Temperatures. *Tribol. Trans.* **1996**, *39*, 787–794.
- (9) Erdemir, A.; Halter, M.; Fenske, G. R.; Zuiker, C.; Csencsits, R.; Krauss, A. R.; Gruen, D. M. Friction and Wear Mechanisms of Smooth Diamond Films During Sliding in Air and Dry Nitrogen. *Tribol. Trans.* **1997**, *40*, 667–675.
- (10) Donnet, C. Recent progress on the tribology of doped diamond-like and carbon alloy coatings: a review. *Surf. Coat. Technol.* **1998**, *100*, 180–186.
- (11) Grillo, S. E.; Field, J. E. *Friction Natural CVD Diamond Wear* **2003**, *254*, 945–949.
- (12) Grill, A. Diamond-like carbon: state of the art. *Diamond Relat. Mater.* **1999**, *8*, 428–434.
- (13) Hauer, R.; Muller, U. An overview on tailored tribological and biological behavior of diamond-like carbon. *Diamond Relat. Mater.* **2003**, *12*, 171–177.
- (14) Heimberg, J. A.; Wahl, K. J.; Singer, I. L.; Erdemir, A. Superlow friction behavior of diamond-like carbon coatings: Time and speed effects. *Appl. Phys. Lett.* **2001**, *78*, 2449–2451.
- (15) Kim, H. I.; Lince, J. R.; Eryilmaz, O. L.; Erdemir, A. Environmental effects on the friction of hydrogenated DLC films. *Tribol. Lett.* **2006**, *21*, 53–58.
- (16) Wu, X.; Ohana, T.; Tanaka, A.; Kubo, T.; Nanao, H.; Minami, I.; Mori, S. Tribocochemical investigation of DLC coating in water using stable isotopic tracers. *Appl. Surf. Sci.* **2008**, *254* (11), 3397–3402.
- (17) Enke, K.; Dimigen, H.; Hubsch, H. Frictional Properties of diamondlike carbon layers. *Appl. Phys. Lett.* **1980**, *36*, 291–292.
- (18) Donnet, C.; Le Mogne, T.; Ponsonnet, L.; Belin, M.; Grill, A.; Patel, V.; Jahnes, C. The respective role of oxygen and water vapor on the tribology of hydrogenated diamond-like carbon films. *Tribol. Lett.* **1998**, *4*, 259–265.
- (19) Gardoš, M. N. Tribological fundamentals of polycrystalline diamond films. *Surf. Coat. Technol.* **1999**, *113*, 183.
- (20) Tillmann, W.; Vogli, E.; Hoffmann, F. Low-friction diamond-like carbon (DLC)-layers for humid environment. *Thin Solid Films* **2007**, *516*, 262–266.
- (21) Dimigen, H.; Hubsch, H.; Memming, R. Tribological and Electrical Properties of Metal-Containing Hydrogenated Carbon-Films. *Appl. Phys. Lett.* **1987**, *50* (16), 1056–1058.
- (22) Scharf, T. W.; Singer, I. L. Monitoring transfer films and friction instabilities with in situ Raman tribometry. *Tribol. Lett.* **2003**, *14* (1), 3–8.
- (23) Singer, I. L.; Dvorak, S. D.; Wahl, K. J.; Scharf, T. W. Role of third bodies in friction and wear of protective coatings. *J. Vac. Sci. Technol. A* **2003**, *21*, S232–S240.
- (24) Eryilmaz, O. L.; Erdemir, A. TOF-SIMS and XPS characterization of diamond-like carbon films after tests in inert and oxidizing environments. *Wear* **2008**, *265* (1–2), 244–254.
- (25) Fontaine, J.; Belin, M.; Le Mogne, T.; Grill, A. How to restore superlow friction of DLC: the healing effect of hydrogen gas. *Tribol. Int.* **2004**, *37*, 869–877.
- (26) Fontaine, J.; Le Mogne, T.; Loubet, J. L.; Belin, M. Achieving superlow friction with hydrogenated amorphous carbon: some key requirements. *Thin Solid Films* **2005**, *482*, 99–108.
- (27) Donnet, C.; Grill, A. Friction control of Diamond-Like Carbon Coatings. *Surf. Coat. Technol.* **1997**, *94*–*95*, 456–462.
- (28) Erdemir, A. Synthesis of Superlow-Friction Carbon Films from Highly Hydrogenated Methane Plasmas. *Surf. Coat. Technol.* **2000**, *133*–*134*, 448–454.
- (29) Hayward, I. P. Friction and Wear Properties of Diamond and Diamond Coatings. *Surf. Coat. Technol.* **1991**, *49*, 554–559.
- (30) Sumant, A. V.; Grierson, D. S.; Gerbi, J. E.; Birrell, J.; Lanke, U. D.; Auciello, O.; Carlisle, J. A.; Carpick, R. W. Toward the ultimate tribological interface: Surface chemistry and nanotribology of ultrananocrystalline diamond. *Adv. Mater.* **2005**, *17* (8), 1039+.
- (31) Sumant, A. V.; Grierson, D. S.; Gerbi, J. E.; Carlisle, J. A.; Auciello, O.; Carpick, R. W. Surface chemistry and bonding configuration of ultrananocrystalline diamond surfaces and their effects on nanotribological properties. *Phys. Rev. B* **2007**, *76* (23).
- (32) Gao, F.; Erdemir, A.; Tysoe, W. T. The tribological properties of low-friction hydrogenated diamond-like carbon measured in ultrahigh vacuum. *Tribol. Lett.* **2005**, *20* (3–4), 221–227.
- (33) Rabbani, F.; Vogelaar, B. M. The importance of unbound hydrogen and increased aromatic structure on the friction and wear behaviour of amorphous hydrogenated carbon (a-C: H) coatings. *Diamond Relat. Mater.* **2004**, *13* (1), 170–179.
- (34) Zhang, S. L.; Wagner, G.; Medyanik, S. N.; Liu, W. K.; Yu, Y. H.; Chung, Y. W. Experimental and molecular dynamics simulation studies of friction behavior of hydrogenated carbon films. *Surf. Coat. Technol.* **2004**, *177*–*178*, 818–823.
- (35) Gao, G.-T.; Mikulski, P. T.; Chateauneuf, G. M.; Harrison, J. A. The Effects of Film Structure and Surface Hydrogen on the Properties of Amorphous Carbon Films. *J. Phys. Chem. B* **2003**, *107*, 11082–11090.
- (36) Gao, G. T.; Mikulski, P. T.; Harrison, J. A. Molecular-Scale Tribology of Amorphous Carbon Coatings: Effects of Film Thickness, Adhesion, and Long-Range Interactions. *J. Am. Chem. Soc.* **2002**, *124*, 7202–7209.
- (37) Harrison, J. A.; Colton, R. J.; White, C. T.; Brenner, D. W. Atomistic Simulation of the Nanoindentation of Diamond and Graphite Surfaces. *Mater. Res. Soc. Symp. Proc.* **1992**, *239*, 573–578.
- (38) Harrison, J. A.; Brenner, D. W.; White, C. T.; Colton, R. J. Atomistic Mechanisms of Adhesion and Compression of Diamond Surfaces. *Thin Solid Films* **1991**, *206* (1–2), 213–219.
- (39) Dag, S.; Ciraci, S. Atomic scale study of superlow friction between hydrogenated diamond surfaces. *Phys. Rev. B* **2004**, *70* (24).
- (40) Erdemir, A.; Eryilmaz, O. L.; Fenske, G. R. Synthesis of diamond-like carbon films with superlow friction and wear properties. *J. Vac. Sci. Technol. A* **2000**, *18*, 1987–1992.
- (41) Chromik, R. R.; Winfrey, A. L.; Luning, J.; Nemanich, R. J.; Wahl, K. J. Run-in behavior of nanocrystalline diamond coatings studied by in situ tribometry. *Wear* **2008**, *265* (3–4), 477–489.
- (42) Konicek, A. R.; Grierson, D. S.; Gilbert, P.; Sawyer, W. G.; Sumant, A. V.; Carpick, R. W. Origin of ultralow friction and wear in ultrananocrystalline diamond. *Phys. Rev. Lett.* **2008**, *100* (23).
- (43) Scharf, T. W.; Singer, I. L. Thickness of diamond-like carbon coatings quantified with Raman spectroscopy. *Thin Solid Films* **2003**, *440* (1–2), 138–144.
- (44) Scharf, T. W.; Singer, I. L. Quantification of the thickness of carbon transfer films using Raman tribometry. *Tribol. Lett.* **2003**, *14* (2), 137–145.
- (45) Sawyer, W. G.; Wahl, K. J. Accessing Inaccessible Interfaces: In Situ Approaches to Materials Tribology. *Mater. Res. Soc. Bull.* **2008**, *33* (12), 1145–1148.
- (46) Wahl, K. J.; Sawyer, W. G. Observing Interfacial Sliding Processes in Solid-Solid Contacts. *Mater. Res. Soc. Bull.* **2008**, *33* (12), 1159–1167.
- (47) Marks, L. D.; Warren, O. L.; Minor, A. M.; Merkle, A. P. Tribology in Full View. *Mater. Res. Soc. Bull.* **2008**, *33* (12), 1168–1173.
- (48) Merkle, A. P.; Marks, L. D. Friction in full view. *Appl. Phys. Lett.* **2007**, *90* (6).
- (49) Harrison, J. A.; Gao, G.; Schall, J. D.; Knippenberg, M. T.; Mikulski, P. T. Friction between solids. *Philos. Trans. R. Soc. a-Math. Phys. Eng. Sci.* **2008**, *366* (1869), 1469–1495.
- (50) Harrison, J. A.; Schall, J. D.; Knippenberg, M. T.; Gao, G.; Mikulski, P. T. Elucidating Atomic-Scale Friction using MD and Specialized Analysis Techniques. *J. Phys.: Condens. Matter* **2008**, *20*, 354009.
- (51) Lupkowski, M.; van Swol, F. J. *Chem. Phys.* **1990**, *93*, 737.

- (52) Chandross, M.; Grest, G. S.; Stevens, M. J. Friction between Alkylsilane Monolayers: Molecular Simulation of Ordered Monolayers. *Langmuir* **2002**, *18*, 8392–8399.
- (53) Perry, M. D.; Harrison, J. A. Universal Aspects of the Atomic-Scale Friction of Diamond Surfaces. *J. Phys. Chem.* **1995**, *99*, 9960–9965.
- (54) Swope, W. C.; Andersen, H. C.; Berens, P. H.; Wilson, K. R. *J. Chem. Phys.* **1982**, *76*, 637–649.
- (55) Adelman, S. A.; Doll, J. D. Generalized Langevin Equation Approach for Atom/Solid-Surface Scattering: General Formulation of Classical Scattering off Harmonic Solids. *J. Chem. Phys.* **1976**, *64*, 2375–2388.
- (56) Verlet, L. *Phys. Rev. B* **1967**, *159*, 98.
- (57) Brenner, D. W.; Shenderova, O. A.; Harrison, J. A.; Stuart, S. J.; Ni, B.; Sinnott, S. B. Second Generation Reactive Empirical Bond Order (REBO) Potential Energy Expression for Hydrocarbons. *J. Phys. C* **2002**, *14*, 783–802.
- (58) Brenner, D. W. Empirical Potential for Hydrocarbons for use in Simulating Chemical Vapor Deposition of Diamond Films. *Phys. Rev. B* **1990**, *42*, 9458–9471.
- (59) Brenner, D. W.; Harrison, J. A.; White, C. T.; Colton, R. J. Molecular-Dynamics Simulations of the Nanometer-Scale Mechanical-Properties of Compressed Buckminsterfullerene. *Thin Solid Films* **1991**, *206* (1–2), 220–223.
- (60) Trotter, H.; Phillips, R.; Ni, B.; Hu, Y. H.; Sinnott, S. B.; Mikulski, P. T.; Harrison, J. A. Effect of filling on the compressibility of carbon nanotubes: Predictions from molecular dynamics simulations. *J. Nanosci. Nanotechnol.* **2005**, *5* (4), 536–541.
- (61) Yakobson, B. I.; Brabec, C. J.; Bernholc, J. Nanomechanics of carbon tubes: Instabilities beyond linear response. *Phys. Rev. Lett.* **1996**, *76*, 2511.
- (62) Brenner, D. W.; Dunlap, B. I.; Harrison, J. A.; Mintmire, J. W.; Mowrey, R. C.; Robertson, D. H.; White, C. T. Group IV Covalent Clusters: Si45 and C44 vs. Si44 and C45. *Phys. Rev. B* **1991**, *44*, 3479–3482.
- (63) Harrison, J. A.; White, C. T.; Colton, R. J.; Brenner, D. W. Molecular-dynamics simulations of atomic-scale friction of diamond surfaces. *Phys. Rev. B* **1992**, *46*, 9700–9708.
- (64) Harrison, J. A.; Colton, R. J.; White, C. T.; Brenner, D. W. Effect of atomic-scale roughness on friction: A molecular dynamics study of diamond surfaces. *Wear* **1993**, *168*, 127–133.
- (65) Harrison, J. A.; Brenner, D. W. Simulated Tribochimistry: An Atomic-Scale View of the Wear of Diamond. *J. Am. Chem. Soc.* **1994**, *116*, 10399–10402.
- (66) Harrison, J. A.; Stuart, S. J.; Brenner, D. W. Atomic-Scale Simulation of Tribological and Related Phenomena. In *Handbook of Micro/Nanotribology*, 2nd ed.; Bhushan, B., Ed.; CRC Press: Boca Raton, FL, 1999; pp 525–594.
- (67) Harrison, J. A.; White, C. T.; Colton, R. J.; Brenner, D. W. Molecular Dynamics Simulations of the Atomic Scale Friction of Diamond Surfaces. *Phys. Rev. B* **1992**, *46*, 9700–9708.
- (68) Harrison, J. A.; White, C. T.; Colton, R. J.; Brenner, D. W. Effects of Chemically-Bound, Flexible Hydrocarbon Species on the Frictional Properties of Diamond Surfaces. *J. Phys. Chem.* **1993**, *97*, 6573–6576.
- (69) Harrison, J. A.; White, C. T.; Colton, R. J.; Brenner, D. W. Investigation of the Atomic-scale Friction and Energy Dissipation in Diamond using Molecular Dynamics. *Thin Solid Films* **1995**, *260*, 205–211.
- (70) Shenderova, O. A.; Brenner, D. W. Atomistic simulations of structures and mechanical properties of <011> tilt grain boundaries and their triple junctions in diamond. *Phys. Rev. B* **1999**, *60* (10), 7053–7061.
- (71) Shenderova, O. A.; Brenner, D. W. Atomistic simulation of grain boundaries, triple junctions and related disclinations. *Solid State Phenom.* **2002**, *87*, 205.
- (72) Stuart, S. J.; Tutein, A. B.; Harrison, J. A. A Reactive Potential for Hydrocarbons with Intermolecular Interactions. *J. Chem. Phys.* **2000**, *112*, 6472–6486.
- (73) Jager, H. U.; Albe, K. Molecular-dynamics simulations of steady-state growth of ion-deposited tetrahedral amorphous carbon films. *J. Appl. Phys.* **2000**, *88*, 1129–1135.
- (74) Kaukonen, H.-P.; Nieminen, R. M. Molecular-Dynamics Simulations of the Growth of Diamondlike Films by Energetic Carbon-Atom Beams. *Phys. Rev. Lett.* **1992**, *68*, 620–623.
- (75) Kohary, K.; Kugler, S. Growth of Amorphous Carbon: Molecular Dynamics Simulation of Atomic Bombardment. *Phys. Rev. B* **2001**, *63*, 292–297.
- (76) Bilek, M. M. M.; McKenzie, D. R.; McCulloch, D. G.; Gorringe, C. M. Ab initio simulation of structure in amorphous hydrogenated carbon. *Phys. Rev. B* **2000**, *62*, 3071–3077.
- (77) Glosli, J. N.; Ree, F. H. Liquid-liquid phase transformation in carbon. *Phys. Rev. Lett.* **1999**, *82*, 4659–4662.
- (78) Marks, N. A. Generalizing the environment-dependent interaction potential for carbon. *Phys. Rev. B* **2000**, *63*, 035401-1–035401-7.
- (79) Marks, N. A.; Cooper, N. C.; McKenzie, D. R. Comparison of density-function, tight-binding, and empirical methods for the simulation of amorphous carbon. *Phys. Rev. B* **2002**, *65*, 075411-1–075411-9.
- (80) Marks, N. A.; McKenzie, D. R.; Pailthorpe, B. A.; Bernasconi, M.; Parrinello, M. Microscopic Structure of Tetrahedral Amorphous Carbon. *Phys. Rev. Lett.* **1996**, *76*, 768–771.
- (81) McCulloch, D. G.; McKenzie, D. R.; Gorringe, C. M. Ab initio simulations of the structure of amorphous carbon. *Phys. Rev. B* **2000**, *61*, 2349–2355.
- (82) Ferrari, A. C.; Robertson, J. Interpretation of Raman spectra of disordered and amorphous carbon. *Phys. Rev. B* **2000**, *61* (20), 14095–14107.
- (83) Stark, P. A. *Introduction to Numerical Recipes*; MacMillian: Toronto, 1970.
- (84) Wahl, K. J.; Chromik, R. R.; Lee, G. Y. Quantitative in situ measurement of transfer film thickness by a Newton's rings method. *Wear* **2008**, *264* (7–8), 731–736.
- (85) Feng, Z.; Tzeng, Y.; Field, J. E. Friction of Diamond on Diamond in Ultra-High Vacuum and Low-Pressure Environments. *J. Phys. D-Appl. Phys.* **1992**, *25* (10), 1418–1424.
- (86) Gardos, M. N.; Soriano, B. L. The Effect of Environment on the Tribological Properties of Polycrystalline Diamond Films. *J. Mater. Res.* **1990**, *5* (11), 2599–2609.
- (87) Gardos MN, G. S. Atmospheric effects of friction, friction noise and wear with silicon and diamond. Part III. SEM tribometry of polycrystalline diamond in vacuum and hydrogen. *Tribol. Lett.* **1999**, *6*, 103–112.
- (88) Grillo, S. E.; Field, J. E. The friction of CVD diamond at high Hertzian stresses: the effect of load, environment and sliding velocity. *J. Phys. D-Appl. Phys.* **2000**, *33* (6), 595–602.
- (89) Erdemir, A. The role of hydrogen in tribological properties of diamond-like carbon films. *Surf. Coat. Technol.* **2001**, *146*, 292–297.
- (90) Harrison, J. A.; White, C. T.; Colton, R. J.; Brenner, D. W. Nanoscale Investigation of Indentation, Adhesion and Fracture of Diamond (111) Surfaces. *Surf. Sci.* **1992**, *271* (1–2), 57–67.
- (91) Perry, M. D.; Harrison, J. A. Universal Aspects of the Atomic-scale Friction of Diamond Surfaces. *J. Phys. Chem.* **1995**, *99*, 9960–9965.

JP904871T